Chapter 10
Flooding Hazard Assessment Considering Climate Change in the Coastal Areas of Algeria Based on a Remote Sensing and GIS Data Base

Barbara Theilen-Willige and Rachid Mansouri

Abstract Evaluations of satellite data, geophysic, bathymetric and meteorologic data as well as digital elevation data, help to identify critical coastal areas in N-Algeria exposed to flooding due to flash floods, storm surge, meteo-tsunamis or tsunami waves. Data mining is the prerequisite for flooding hazard preparedness. It is aiming at visualizing critical areas and providing information about damage in case of emergency due to flooding hazards as fast as possible, as the civil protection units need this information for their management. The actual inventory of land use and infrastructure (bridges, railroads, roads, river embankments, etc.), industrial facilities and the structure of settlements and cities is an important issue for the hazard assessment and damage loss estimation.

Sea level rise due to climate change has to be considered when dealing with the detection of areas susceptible to flooding. Evaluations of optical satellite data such as Landsat 8 and Sentinel 2 and radar data (Sentinel 1, ALOS PALSAR) contribute to a better understanding of the development of currents at the coast and their interactions with the coastal morphology. A systematic inventory of coast segments showing traces of flooding in the past is presented as well as the monitoring of coast-near lowlands, lakes and ponds. Digital elevation model (DEM) including bathymetric data help to identify areas prone to flooding.

Keywords Remote sensing · GIS · Flooding hazard · Tsunamis · Sturm surge · Flash floods · N-Algeria

B. Theilen-Willige (✉)
TU Berlin, Berlin, Germany
e-mail: barbara.theilen-willige@campus.tu-berlin.de

R. Mansouri
Department of Civil Engineering and Hydraulics, Laboratory LGCH, 8 Mai 1945 Guelma University, Guelma, Algeria
e-mail: mansouri.rachid@univ-guelma.dz

10.1 Introduction

The Algerian coast has been prone to hazardous tsunamis as Northern Algeria is located at the boundary between the African and European plates. The convergence rate between those tectonic plates is in the range of order of 4–7 mm per year (Amir & Theilen-Willige, 2017). The compressive motion results in the occurrence of tsunamogenic earthquakes in Western Mediterranean, in particular, the Alboran Sea separating the Ibero area in Spain and Maghreb in Morocco and Western part of Algeria (Fig. 10.1). On October 1790, a devastating earthquake hit Oran city in North Western of Algeria (Io = IX − X, MSK Scale). Historical spanish documents reports that two thousand people died in North Africa (Lopez Marinas & Salord, 1990). The seismic crisis consisted of a series of foreshocks reported during September and beginning of October 1790. The main shock occurred at 01:15 AM on the ninth of October and aftershocks are reported until February 1790. The earthquake was felt as far as 200 km from Oran to Almeria and Carthagena in southern Spain. A tsunami was generated just a few minutes after the main shock. In the Algerian coast, the sea withdrawal was about 200 m. In Spain, the sea penetrated inland by 50 m nearby Almeria. In the harbour of Carthagena the sea rose by 1.8 m (Lopez Marinas & Salord, 1990). Tsunami water waves in the Oran, Arzew and
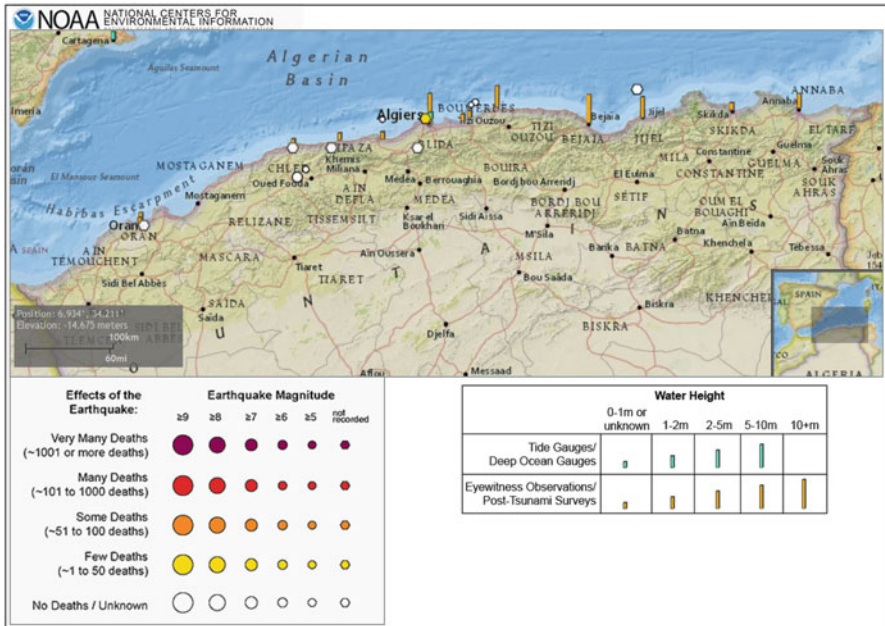

Fig. 10.1 Tsunami events along the Algerian coast
NOAA Web Map https://maps.ngdc.noaa.gov/viewers/hazards/?layers=0

Almeria Bay were trapped along the coasts for a long time. The tsunami propagation in the Alboran Sea lasted about an hour (Amir et al., 2012; Amir, 2014).

The Djidjelli Earthquake of August 21 and 22, 1856 triggered sea waves of 2–3 m high (observed at Djidjelli) that flooded the eastern Algerian coast several times. At Bougie (Bejaia) and Philippeville (Skikda), small towns located eighty kilometers west and east of Djidjelli, Ambraseys & Vogt (1988) and Soloviev et al. (2000) reported that the sea rose from about 5 m, flooding the shore five to six times (Yelles-Chaouche et al., 2009).

During the instrumental period, two tsunamigenic events are evidenced as they were the first recorded by geophysical instruments. The first one occurred after the destructive El Asnam event of October 10, 1980 (Ms: 7.3). Although located at a distance of about 60 km from the coast, the earthquake triggered a submarine landslide inducing a weak tsunami recorded by several tide gauge stations of southeastern Spain (Papadopoulos & Fokaefs, 2005). The second tsunami, the more recent one, is the tsunami of Boumerdes of 21.05.2003. This event, one of the most important in the western Mediterranean region within the last century, was generated by an earthquake of magnitude Mw 6.8 that occurred on the offshore reverse fault of Zemmouri (Yelles et al., 2004; Alasset et al., 2006). This thrust fault, with a length of about 50–55 km, is assumed to outcrop near the seafloor at about 10–15 km from the shoreline (Deverchere et al., 2005). Effects of this tsunami were felt in the entire westernnMediterranean region and especially along the Balearic coasts (Alasset et al., 2006). The Boumerdes tsunami demonstrated the high potential of the Algerian margin for tsunami generation (Yelles-Chaouche et al., 2009), see Fig. 10.1.

The main cause of tsunami generation in the Mediterranean Sea is tectonic activity associated with strong earthquakes. However, tsunami waves are also generated by landslides. Most of them were caused by subaerial landslides or marine slides induced mainly by earthquakes and less frequently by volcanic eruptions. For the vast majority of volcanic events the actual generation mechanism of destructive water waves is a volcanic slope failure (Gusiakov, 2020). Several types of landslides cause tsunamis with significant heights in near-source coasts that attenuate rapidly due to frequency dispersion (Papadopoulos et al., 2007). Due to the concentrated large wave heights, such tsunamis may result in catastrophic consequences. The magnitude 6.8 earthquake (21.05.2003) located near Boumerdes (central Algerian coast) triggered large turbidity currents responsible for 29 submarine cable breaks at the foot of the continental slope over 150 km from west to east (Cattaneo et al., 2012).

When dealing with the flooding hazard potential along the Algerian coasts it is necessary to consider meteotsunamis as well, see as an example Fig. 10.2. Meteotsunamis caused by extreme weather events and storm surge can affect coastel areas with increasing intensity due to the effects of climate change. Meteotsunamis are much less energetic than seismic tsunamis and that is why they are occurring local, similar to landslide tsunamis. Destructive meteotsunamis are always the result of a
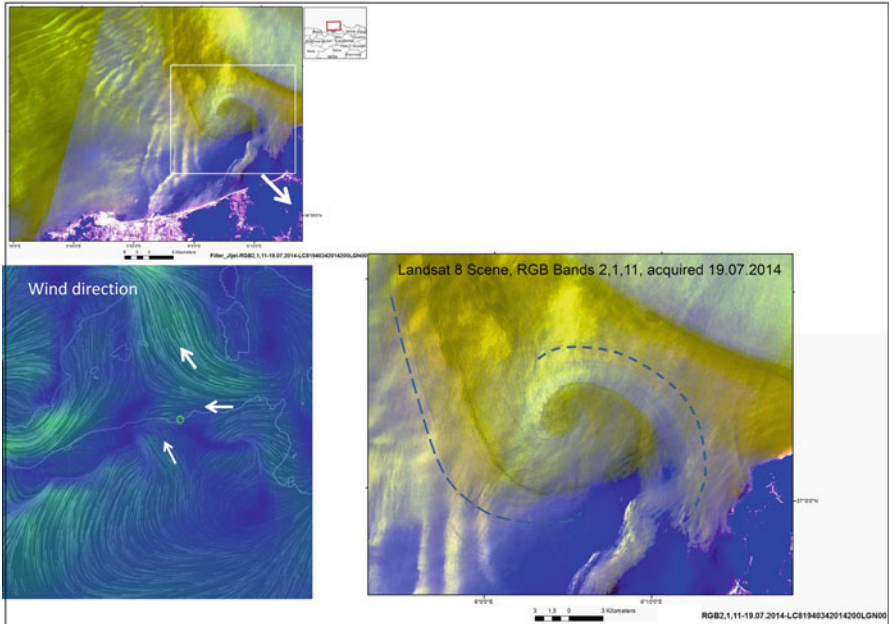
Fig. 10.2 Surface water current development (Landsat 8, 19.07.2014) near the city of Jijel east of Algiers
There were no clouds, fog or mist at the acquisition time. The wave pattern visible on the image is related to the water surface current pattern at the acquisition time (correlated with data from https://earth.nullschool.net)

combination of several resonant factors (atmospheric gravity waves, pressure jumps, frontal passages, squalls, etc.). The low probability of such a combination is the main reason why major meteotsunamis are infrequent and observed only at some specific locations (Monserrat et al., 2006).

As extreme weather events will increase due to climate change the occurrence of extreme sea level oscillations associated with meteotsunamis and storm surge will be an important issue at the Algerian coast.

The sea level rise related to climate change has to be taken into account as well when dealing with the detection of areas prone to potential tsunami flooding. Climate models project a Global mean sea level (GMSL) rise during the twenty-first century that will likely be in the range of 0.29–0.59 m for a low emissions scenario and 0.61–1.10 m for a high one. GMSL projections that include the possibility of faster disintegration of the polar ice sheets predict a rise of up to 2.4 m in 2100 and up to 15 m in 2300 (European Environment Agency, 2021).

How this will affect the tidal range has still to be investigated.

These sea level rise trends have to be considered when dealing with flooding hazard preparedness in coastal areas This means that tsunami flooding modeling has to consider and to include these sea level changes when calculating the potential indundation extent.

10.1.1   The Role of Remote Sensing and GIS

When catastrophic earthquake and tsunami hazards happen and affect cities, settlements and infrastructure, immediate and efficient actions are required which ensure the minimization of the damage and loss of human lives. Proper mitigation of damages following disastrous events highly depends on the available information and the quick and proper assessment of the situation. Responding local and national authorities should be provided in advance with information and maps where the highest damages due to unfavourable, local site conditions in case of stronger flooding events can be assumed. The better a pre-existing reference database of an area at risk is prepared and elaborated, the better a crisis-management can react in case of hazards and related secondary effects. The potential of social and economic losses due to those events is increasing. Therefore, information of geodynamic processes is a basic need for the long-term safety of cities, settlements, infrastructure and industrial facilities. The assessment of potential hazard prone areas is fundamental for planning purposes and risk preparedness, especially with regard to supervision and maintenance of settlements, infrastructure, industrial facilities and of extended lifelines (Amir & Theilen-Willige, 2017).

The ability to undertake the assessment, monitoring and modeling can be improved to a considerable extent through the current advances in remote sensing and GIS technology. Causal or critical environmental factors influencing the disposition to be affected by flooding hazards and the potential damage intensity can be analysed interactively in a GIS database. The interactions and dependencies between different causal and preparatory factors can be visualized and weighted step by step in this GIS environment.

The detection of coastal areas prone to flooding due to torrential rains causing flash floods can be carried out with the support of remote sensing and GIS tools. Flooding can be one of the manageable of natural disasters, if flood prone areas are identified and suitable flood mitigation strategies are implemented. A practical way of identifying flood prone areas is offered by the application of mathematical models, which consider complex hydrological and hydraulic processes of these areas.

Coastal area and river basin management poses big challenges, especially in developing countries, because of lack of continuous data, particularly streamflow data, that require automatic recording instruments to acquire. Remote sensing technology can augment the conventional methods to a great extent in rainfall-runoff studies. The role of remote sensing in runoff calculation is generally to provide a source of input data or it is used as an aid for estimating equation coefficients and model parameters. For example, one of the applications of remote sensing data in hydrologic models is focused on the determination of both, urban and rural land use for estimating runoff coefficients.

10.1.2   Goals of This Study

The aim of this research is focused on a contribution to a coastal hazard geoinformation system with interdisciplinary dynamic content, enabling the communication between local authorities, public organizations and universities. It combines and uses actual and previous efforts by adding new researches, focusing on remote sensing, and new techniques in Geographic Information Systems (GIS). This work could be part of a basic risk assessment presenting information for strategic planning on where potential problems may occur in the infrastructure in the coastal areas of N- Algeria.

This study aims to contribute to the:

- mapping of traces of earlier flooding events on the different satellite images
- influence of different wind directions on current development in the coastal ares and the interaction of currents with the coastal morphology
- delineation of areas prone to flooding due to their morphometric disposition
- evaluation of bathymetric data to analyse the influence of the sea bottom topography on tsunami wave development, especially in the coast-near area
- contribution to a disaster managment system.

10.2   Materials and Methods

The interdisciplinary approach used in the scope of this research comprises remote sensing data, geological, geophysical and topographic data and GIS methods. Earthquake and tsunami data were provided by the European-Mediterranean Seismological Centre (EMSC), International Seismological Centre (ISC), US Geological Survey (USGS) and National Oceanic and Atmospheric Administration (NOAA). Satellite imageries and Digital Elevation Model (DEM) data were used for generating a GIS data base and combined with different geodata and other thematic maps. Satellite data such as Sentinel 1 – C-Band, Synthetic Aperture Radar (SAR) and optical Sentinel 2 images, Advanced Spaceborne Thermal Emission and Reflection Radiometer (ASTER) and Landsat optical data (Landsat TM and Landsat 8, the Operational Land Imager -OLI). Digital Elevation Model (DEM) data gained from the Shuttle Radar Topography Mission (SRTM), ASTER DEM data and Advanced Land Observing Satellite-1 (ALOS), Phased Array type L-band Synthetic Aperture Radar (PALSAR) mission/Japan Aerospace Exploration Agency (JAXA), were downloaded from open-sources such as USGS/Earth Explorer, Sentinel Hub/ESA, Alaska Satellite Facility (ASF) and Google Earth. The data were processed using geoinformation systems ArcGIS from ESRI and QGIS. Shapefiles from Algeria were downloaded from the Geofabrik's download server.

Meteorologic data such as about wind directions and wind speeds were downloaded from the 'power regional data access tool' of the 'POWER Data Access Viewer' provided by NASA as well as from earth.nullschool.net (Beccario, 2020).

10.2.1   Digital Image processing of Different Optical and Radar Satellite Data

ENVI software from Harris Geospatial Solutions and the Sentinel Application Platform (SNAP) provided by ESA were used for the digital image processing of the optical Landsat 5 and 8, Sentinel 2 and ASTER data. SNAP provided as well the tools for the processing of radar data. The evaluation of Sentinel 1 A and B radar images requires geometric correction and calibration.

The different steps of digital image processing used in this research are described in the following text and Fig. 10.3. Digital image processing of LANDSAT 5 Thematic Mapper and Landsat 8 – The Operational Land Imager (OLI) data was carried out by merging different Red Green Blue (RGB) band combinations with the panchromatic Band 8 to pan-sharpen the images. The Red, Green, Blue (RGB)-Principle is reviewed briefly: Three images from different optical satellite bands to be used as end-members in a triplet are projected, one image through one primary color each, one image is coded in blue, the second in green and the third in red.

For the detection of water currents along the Algerian coast various image-processing procedures were tested and the results combined with available meteorological (wind, temperature, etc.) information. Evaluations of LANDSAT, ASTER and Sentinel 2 satellite imageries acquired in time series support a better knowledge of water current dynamics, influenced among other factors (wind direction and speed, upwelling etc.) by the coastal morphology.
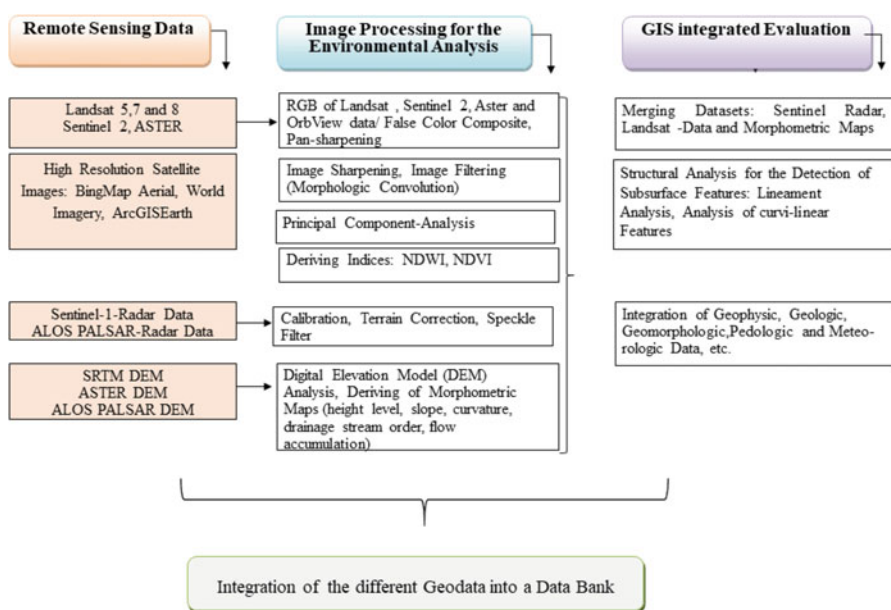

Fig. 10.3 Workflow of the digital data processing

A systematic correlation of the streaming pattern visible on satellite data with wind data, especially wind directions, will contribute to a better understanding of which coastal segments might be prone more to flooding in case of high energetic flood waves from specific directions.

In the scope of this study, the comparative analysis of optical satellite data and the Sentinel 1 radar data was carried out, in order to derive wave pattern and current information. The evaluation of Sentinel 1 A and B radar images requires geometric correction and calibration. The processing of the Sentinel 1 radar data was carried out using the SNAP software of ESA. The illumination geometry of the radar signals in relation to the wind direction plays an important role for the visibility of the water surface properties. Therefore, radar data from descending and ascending orbits with different illumination geometries were used.

10.2.2 Evaluation of Digital Elevation Model (DEM) Data

Digital elevation data help to identify and categorize the different geomorphologic units, their size and arrangement. SRTM, ASTER GDEM (30 m spatial resolution) and Advanced Land Observing Satellite (ALOS), Phased Array type L-band Synthetic Aperture Radar (PALSAR) Digital Elevation Model (12.5 m resolution) were obtained from open sources such as USGS, EarthExplorer and Alaska Satellite Facility (ASF) used with GIS to evaluate terrain features. Terrain features can be described and categorized into simple topographic relief elements or units by parameterizing DEMs such as height levels, slope gradients, and terrain curvature. From DEM (Digital Elevation Model) data derived morphometric maps (slope gradient maps, drainage, etc.) were combined with geologic information in a GIS data base. In the scope of this study DEM data were mainly used to derive information of the lowest and flattest areas prone to flooding in the coastal reas of Algeria

Additionally, the bathymetric DEM data provided by General Bathymetric Chart of the Oceans (GEBCO), International Hydrographic Organization and the Intergovernmental Oceanographic Commission of UNESCO) and EMODnet Bathymetry Consortium (2020) were integrated into the research in order to combine the information of the sea bottom topography with earthquake, tsunami and submarine landslide data (Fig. 10.4).

The integration of different morphometric factors in a GIS environment using weighting procedures plays an important role in the GIS application in the frame of this study. The basic pre-requisite for the use of weighting tools of GIS is the determination of weights and rating values representing the relative importance of factors and their categories. The weighted overlay method takes into consideration the relative importance of the parameters and the classes belonging to each parameter (ESRI, online support in ArcGIS). The application of a weight-linear-
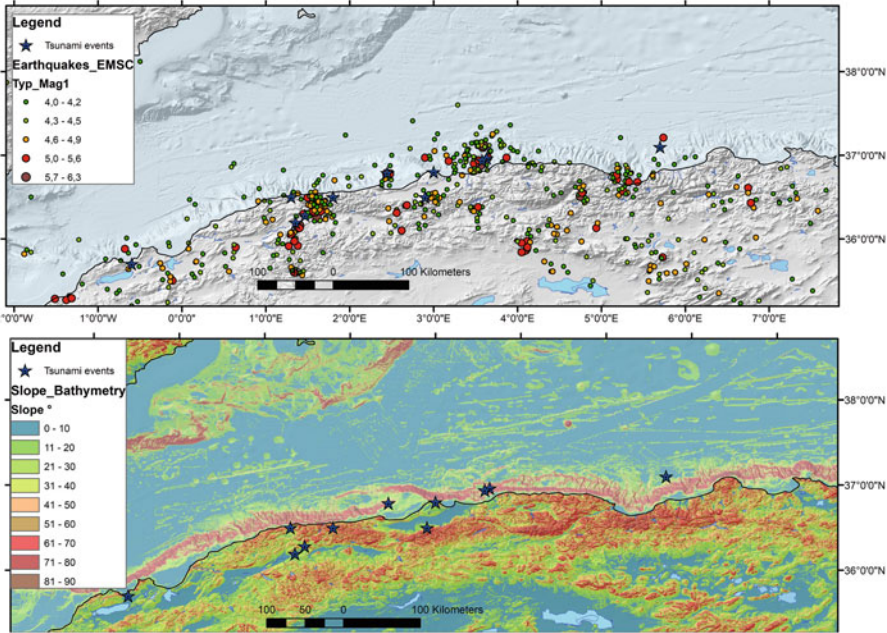
Fig. 10.4 Earthquakes and tsunami events (data sources, EMSC, USGS, ISC, NOAA)
Bathymetric data: GEBCO and EMODnet Bathymetry Consortium

combination in susceptibility assessment has been identified as a semi-quantitative method, involving both expert evaluation and the idea of ranking and weighting factors. The efficacy of the weighted overlay-method lies in the fact that human judgments can be incorporated in the analysis. The weights and ratings are determined using the expert's subjective knowledge. The method starts by assigning an arbitrary weight to the most important criterion (highest percentage), as well as to the least important attribute according to the relative importance of parameters (Fig. 10.5).

The sum over all the causal factors/layers that can be included into GIS provides some information about the susceptibility to flooding and the extent of inundation. This susceptibility is calculated by adding every layer, as described below, to a weighted influence and summing all layers. After weighing (in %) the factors according to their probable influence, susceptibility maps can be elaborated, where those areas are considered as being more susceptible to flooding, where "negative" causal factors occur aggregated and are interfering with each other (Fig. 10.5).
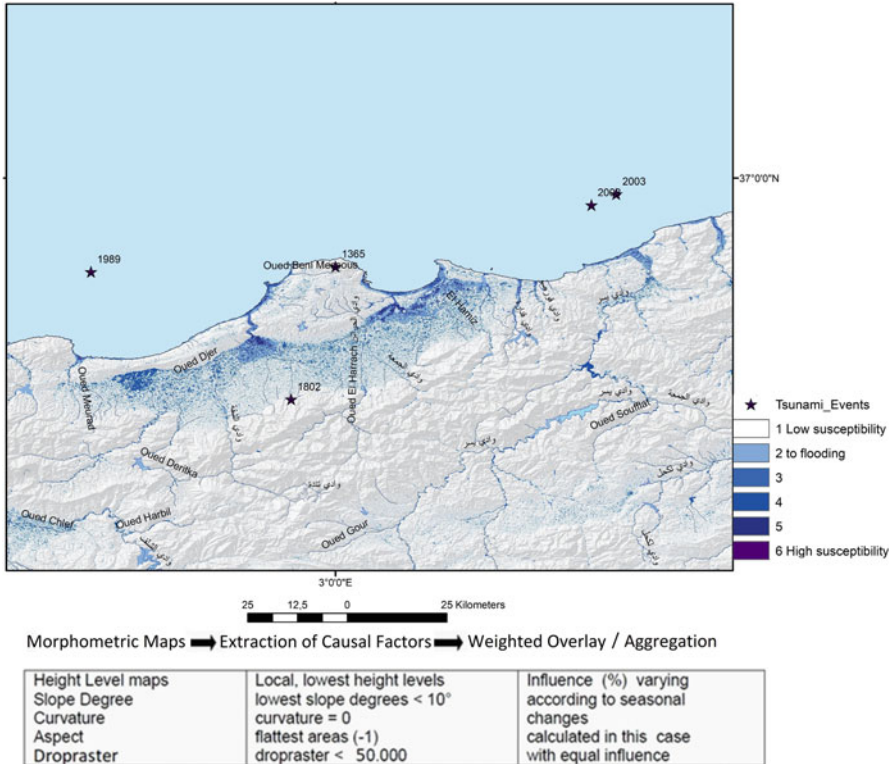
Fig. 10.5 Weighted overlay workflow in ArcGIS to derive information about areas susceptible to flooding due to their morphometric disposition

By extracting first morphometric factors like slope degrees below 10° from the slope gradient map, by deriving from the drop raster the areas with values below 50.000 units using the hydrology-tools in ArcGIS (flow direction), by extracting from curvature maps areas with terrain curvature = 0 and from the aspect map the flat areas (−1), the flattest areas are highlighted. In the weighted overlay procedure these selected morphometric data were summarized, merged with different percentages of influence and represented in a map. The flattest areas with lowest slope degrees and curvatures are classified by values from 0 to 7, thus, enhancing and accentuating the visibility of of areas ptone to flooding

10.3 Results

The direction and angle of incoming, high energetic flood waves will have a significant influence on the water current development, on the interaction with the submarine topography, on the formation of the coastal morphology and on wave dynamics (amplification, interfering). Thus, the wave angles might have an impact on the potential flooding extent in the affected coastal areas. River mouths and their orientation forming an entrance for potential incoming tsunami waves have to be monitored.

The different satellite data and their combined evaluations offer many of the needed information.
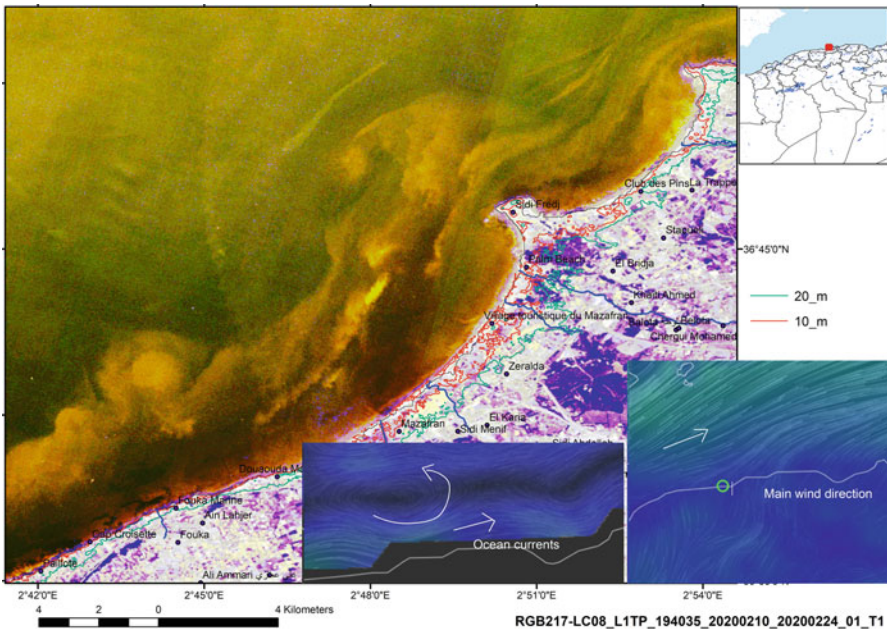
10.3.1 Evaluations of Optical Satellite Data

Optical satellite data of the Algerian coast reveal information of coastal currents (forming coherent water masses in motion) that are found in the region between the coastline and the edge of the continental shelf (Gelfenbaum, 2005).

The exposition to flooding of the coastal segments depends as well on their orientation to the main wave direction and energy.

The next figure shows as an example the water current situation near Jijel on 20.02.2020 (Fig. 10.6). The main wind and water current flow direction was directed towards E-NE (US National Weather Service). Smaller longshore currents can be observed parallel along the arc-shaped coastline. The effects of bottom friction on coastal trapped waves become visible. Every tongue of land or peninsula is causing further currents, depending on the direction of the main wave front.

The sea surface streaming pattern as visible on the Landsat-scenes (only the upper centimeters of the water surface) is mainly influenced by the wind situation at the

Morphometric Maps ➡ Extraction of Causal Factors ➡ Aggregation / Weighted Overlay		
Height Level maps	Local, lowest height levels	Influence (%) varying
Slope Degree	lowest slope degrees < 10°	according to seasonal
Curvature	curvature = 0	changes
Aspect	flattest areas (-1)	calculated in this case
Dropraster	dropraster < 50.000	with equal influence

Fig. 10.6 Water current pattern and wind directions on 10.02.2020 in the Bay of Jijel showing coastal segments exposed to stronger current activity during westwinds (wind and ocean current data from earth: a global map of wind, weather, and ocean conditions, https://earth.nullschool.net/)

acquisition time (wind direction, wind speed), further on by the tidal situation and the input of river water.

Upwelling and downwelling occurs along coastlines, depending on the main wind directions. However, these up-and downwelling processes cannot be monitored directly by remote sensing due to the low penetration depth of the sensors only up to several centimeters. Thermal bands of Landsat 8 and ASTER help to identify current patterns that might be related to these currents.

Satellite images can be used to derive information on water currents and coastal sediment flow dynamics after earthquakes and tsunami events: As the magnitude Boumerde- 6.8 earthquake (21.05.2003) struck at 17:44 local time (USGS, 2003), submarine mass movements and higher sediment discharge of the rivers into the sea had an influence on the water dynamics (Fig. 10.7).

Tsunami-induced morphological changes on coasts prone to inundation and sediment transport changes are controlled by the specific tsunami event and sediment characteristics,

The evaluations of Landsat data reveal that especial semicircular bays are affected by circular currents such as the Bay of Oran, Arzew, Algiers or Bejaia. In case of a stronger tsunami event circular currents could occur in these semicircular bays and, thus, amplify the intensities by interfering and superimposing of wave energy.
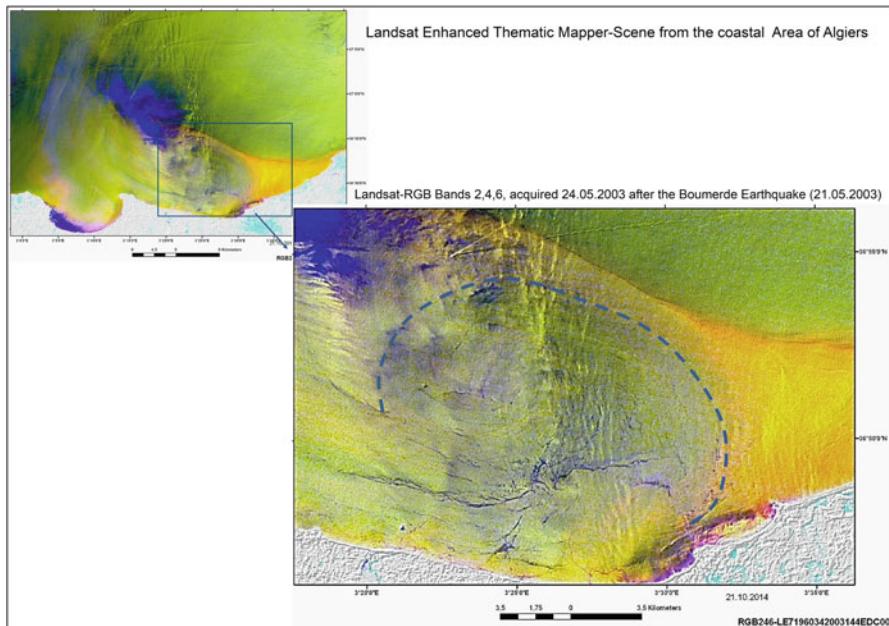

Fig. 10.7 Sediment input (dark-yellow) after the Boumerdes earthquake (21.05.2003) as visible on a Landsat satellite scene

The magnitude 6.8 earthquake struck at 17:44 local time (USGS, 2003), wreaking extensive damage throughout five provinces. Submarine mass movements and higher sediment discharge of the rivers into the sea had an influence on the water dynamics
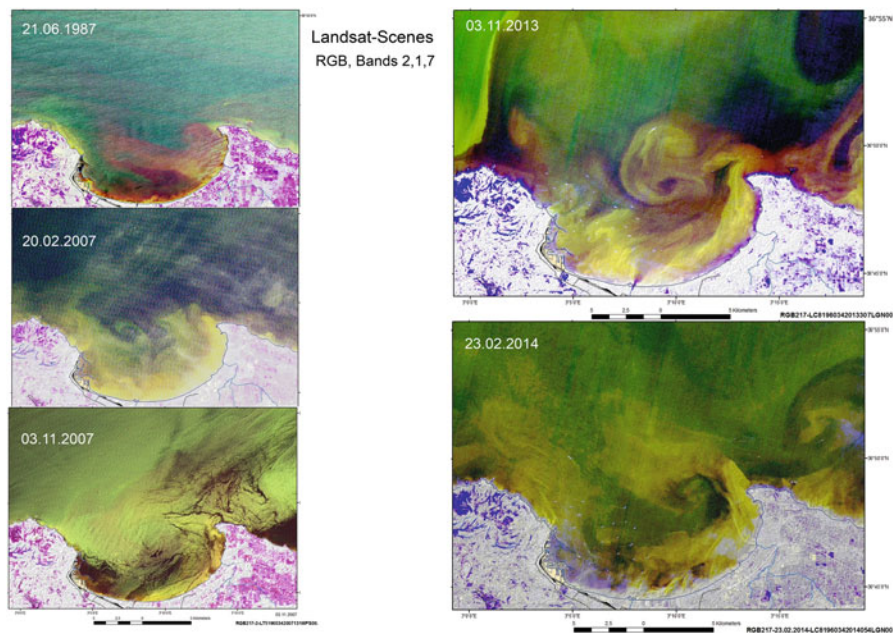
Fig. 10.8 Development of water currents depending on the specific meteorologic conditions and tide situations at the acquisition time of the Landsat data from the Bay of Algiers

The development of the semicircular shaped Bay of Algiers could be explained by such circular streaming dynamics with the consequence of erosional effects as well. The sea surface streaming pattern as visible on the Landsat- and RapidEye-scenes of the Bay of Algiers (visualizing the situation only of the upper centimeters) is mainly influenced by the wind situation at the acquisition time, further on by the tidal situation and the input of river water. This is revealed very clearly by a Landsat time series (Fig. 10.8).

In case of stronger tsunami events with several tsunami wave fronts circular currents might occur in the Bay of Algiers as well and, thus, amplify the intensities by interfering and superimposing of incoming waves. The direction and angle of incoming, high energetic flood waves will have a great influence on the currents and dynamics.

In the next figures different wind situations are presented combined with the current situation at the same time. Figure 10.9 shows the west-wind, Fig. 10.10 the eastwind and Figs. 10.11a and 10.11b the north-wind situation.

The current pattern according to the specific wind directions and wind properties and the interactions with the coastal morphology help to understand which coastal segments might be more affected in case of high energetic waves directed towards the coast. In case of north-winds larger currents could be observed in the semicircle bays along the Algerian coast such as in the Bay of Algiers (Fig. 10.11b).
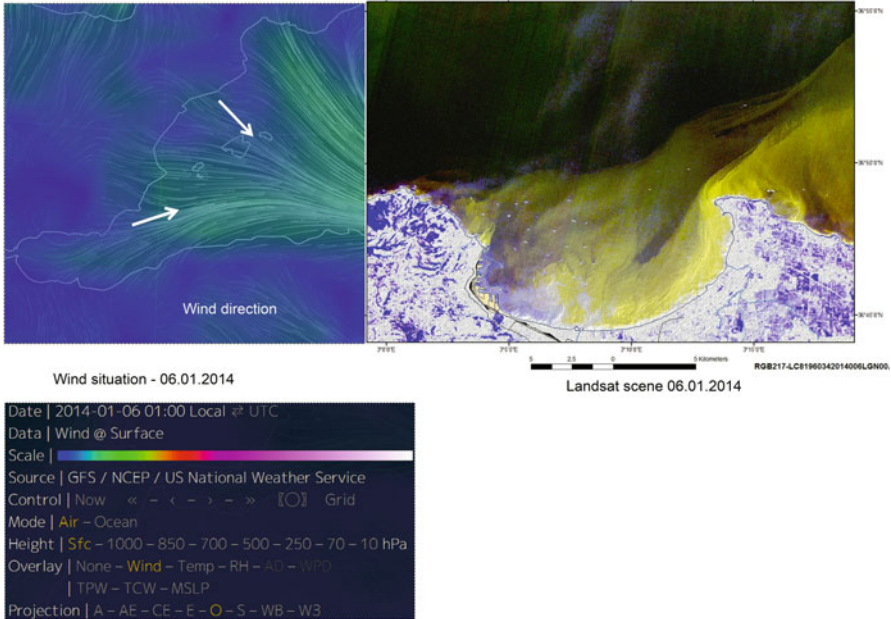
Fig. 10.9 Landsat scene (RGB, Bands 2,1,7, 06.01.2014) showing a west-wind situation
In case of high energetic waves coming from western direction the coast segments oriented more towards these waves would be prone to a higher flooding exposure. Wind data: http://earth.nullschool.net/#2014/02/23/1800Z/wind/surface/level/orthographic=-355.92,38.50,3000

10.3.2 Evaluations of Radar Data

Sentinel 1 synthetic aperture radar (SAR) has been used to detect wave information in a large coverage of the coastal areas of Algeria. Wave parameters such as significant wave height and mean wave period, can be usually obtained from SAR-derived wave spectra (Pleskachevsky et al., 2019; Shao et al., 2016). The evaluation of wave spectra needs a good understanding of complicated SAR wave imaging mechanisms. The C-band VV- and HV polarization Sentinel-1 SAR images are an additional tool whenever cloud cover is a hindrance, provided that the wind properties allow the detection of currents, see Fig. 10.12.

The differences in brightness between pixels in the radar image, marked by changes in the gray scale and backscatter intensity due to surface roughness changes contribute to the detection of wave properties. Dark-blue image tones of the colour-coded radar scene (Fig. 10.12) are associated with low waves because the incident radar signals were largely reflected from their "radar-smooth" surfaces in a mirror-like fashion away from the satellite antenna. High wave areas appear in lighter tones (here in blue-green) as their more radar-rough surfaces generate a diffuse and stronger signal return/radar backscatter. Coast near currents become clearly visible.
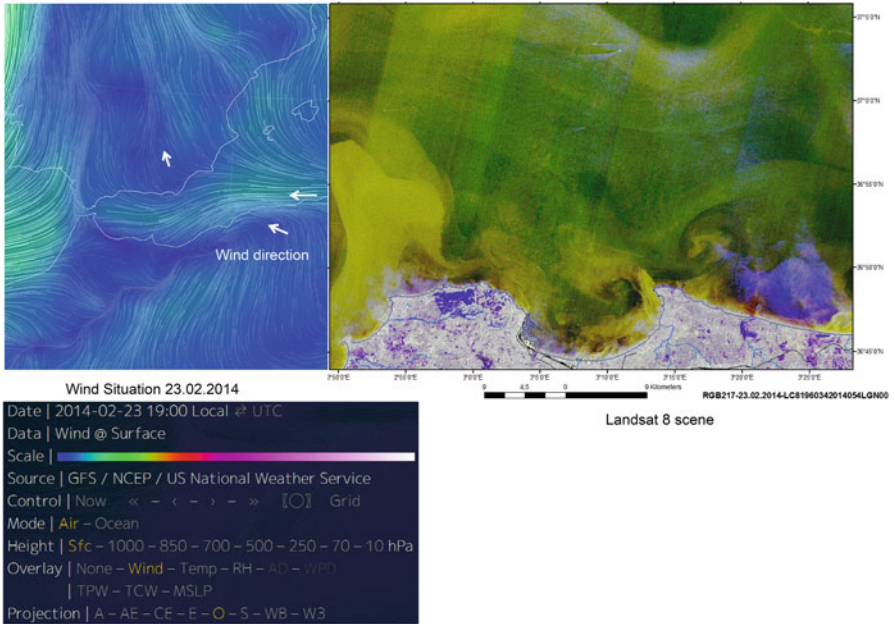
Fig. 10.10 East-wind and water current situation at the coast of Algiers on 23.02.2014
Wind direction data: http://earth.nullschool.net/#2014/02/23/1800Z/wind/surface/level/
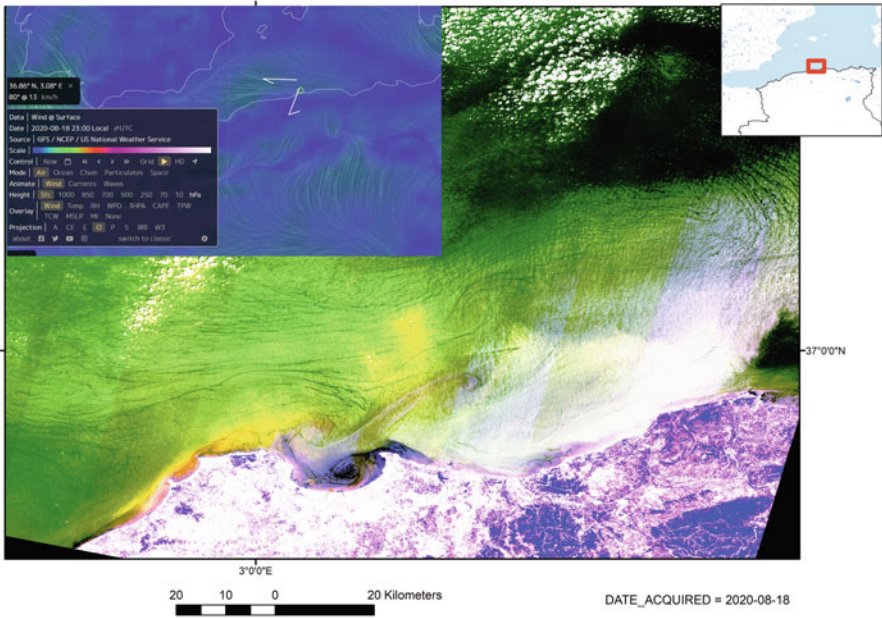orthographic=5.07,36.54,3000

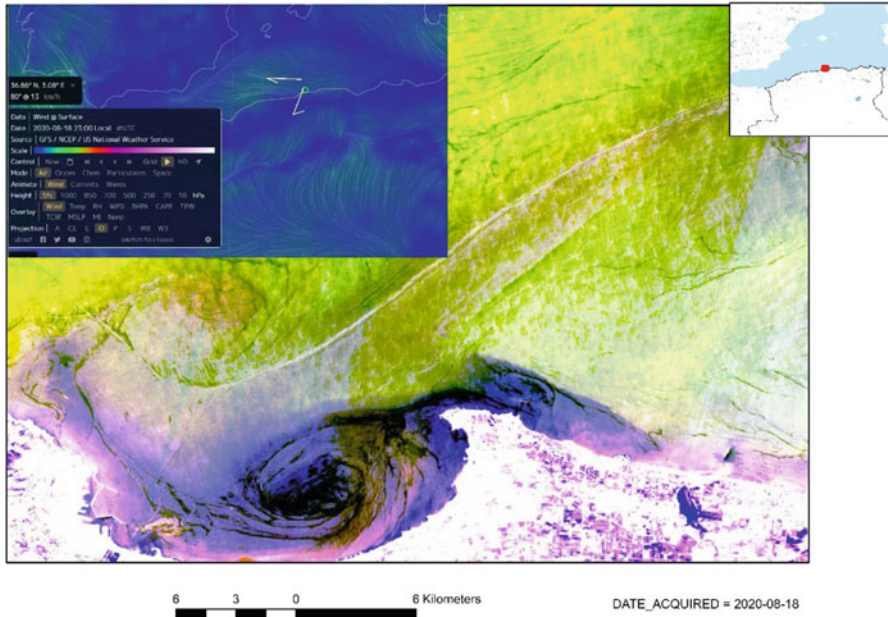**Fig. 10.11a** Current pattern influenced by east to northeast-winds on 18.08.2020

Fig. 10.11b Amplification of Fig. 10.11a: Northern wind direction causing circular coastal currents in the semicircular Bay of Algiers

10.3.3 Evaluations of DEM Data in Combination with Other Satellite Data

A flooding susceptibility map and a potential tsunami hazard map of coastal areas, that predicts the probable locations of possible future inundation and tsunami occurrences, is required which takes into consideration as well the potential morphodynamic consequences of these events at the coasts such as, abrasion, sedimentation and landslides. Undercutting the slopes at the coasts by abrasion and erosion those flood waves initiate a high potential of slope failure.

DEM data help to identify those areas that are most likely to be flooded in case of extreme weather constellations by flash floods or in case of tsunami events which coastal areas might be affected due to their morphometric disposition.

The amount of the sea level rise is still in discussion and in research. In a worst case scenario it will comprise about several meters as mentioned before. Therefore, flooding susceptibility maps of coastal areas should include the future sea level rise. Based on the current free available DEM data the areas below 10 m height level are delineated to show which areas might be prone in future to flooding, wether by sea level rise, sturm surge or by flash floods.

As river mouths are forming an entrance for intruding water waves from the sea a systematic assessment of larger river mouths prone to flooding will contribute to hazard preparedness.
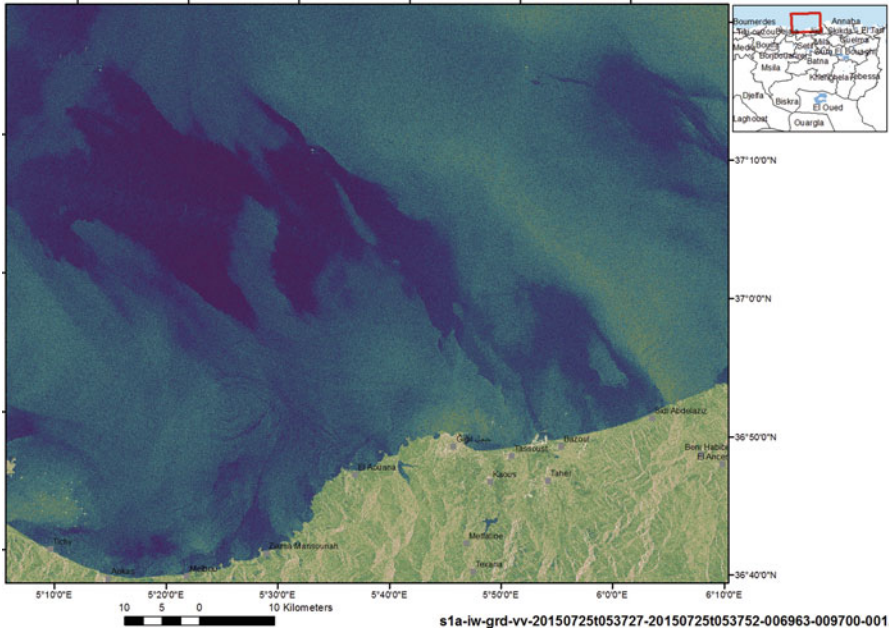
Fig. 10.12 Sentinel-1- Satellite Radar Scene
The dark-blue areas correspond to sea-surfaces with radar-smooth backscatter (mirror-like reflection) related to lower wave heights, the light blue-green areas are related to stronger radar reflection due to higher waves

Further on, the inventory of traces of former sea water intrusion is another important step towards the delineation of coastal segments prone to flooding. Figure 10.13 presents the area of Mersat El Hadjadi (Theilen-Willige, 2006). On the SRTM based morphometric maps and the corresponding Landsat scene traces of former flooding are evident. In case of storm surge or tsunami events it is important to know where the backwater areas are situated which might remain longer flooded after sea waves intrusions and return flow.

Tsunami inundation and damage was not uniform along the Algerian coast in the past. Evaluations of satellite data reveal that coast segments with SSW-NNE to SW-NE orientation have been affected in the past by strong, high energetic sea waves more than W-E oriented coast segments. Most of the latter are steep, cliff coast. The SW-NE orientated sections can be find often within the eastern part of larger semi-circular bay segments.

The affected coast segments that could be identified are shown in Fig. 10.14. Some more detailed views are presented in the Figs.10.15 and 10.16. Due to the coverage by settlements and cities in some sections traces of sea water intrusions cannot be observed on satellite images.

Wave traces of parallel, arrow-shaped debris walls, partly modified by eolian overprint, like in the area of Qued Lekbir in the east of the city of Skikda, are visible
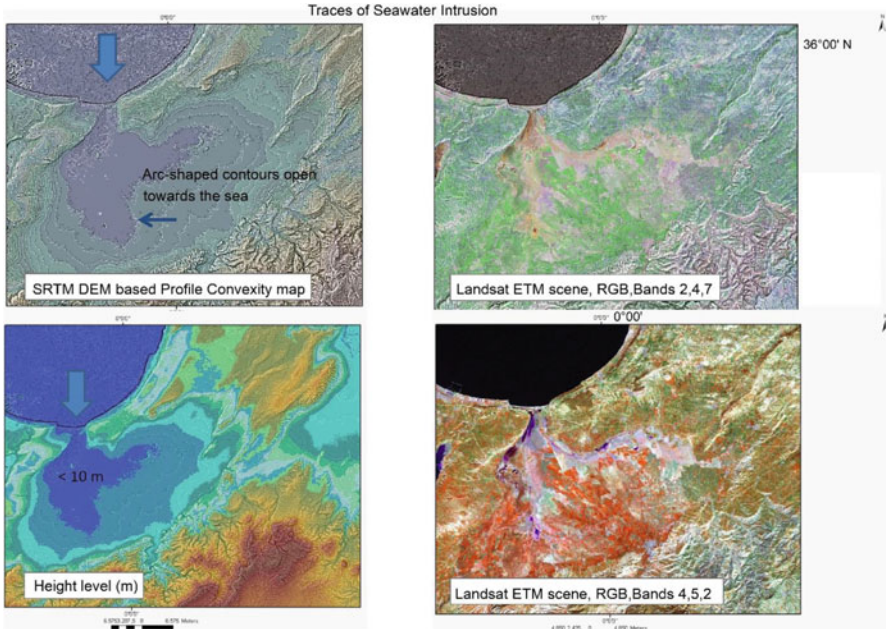
Fig. 10.13 River mouth forming an entrance for flood waves at Mersat El Hadjadj
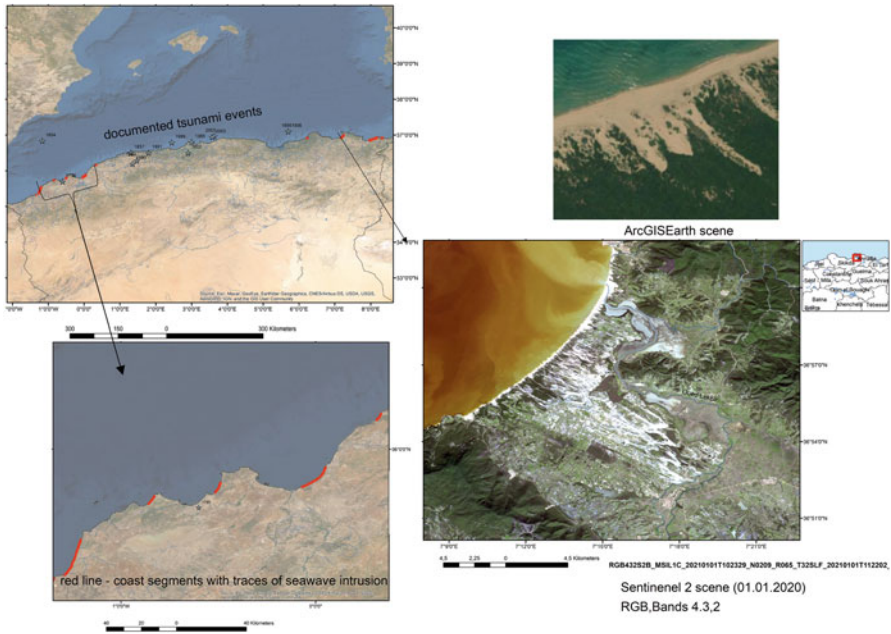

Fig. 10.14 Affected coast segments (red line) by sea wave intrusions, partly along river beds
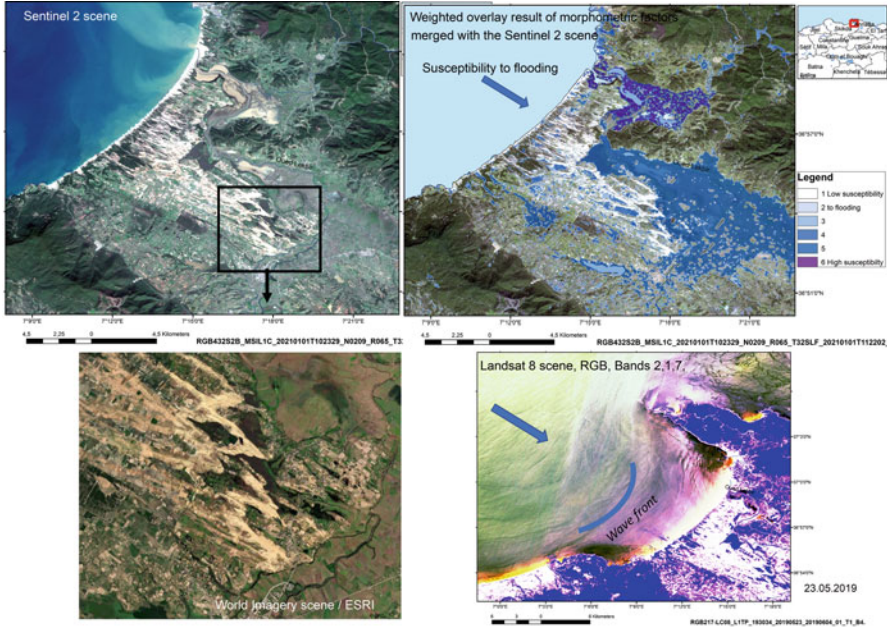
Fig. 10.15 Traces of high energetic flood waves visible on a Sentinel 2 (RGB, Bands 4,3,2) scene and on a Landsat 8 scene (RGB, Bands 2,1,7), modified by eolian activity from the Qued Lebkir east of Skikda, NE-Algeria
The weighted overlay of morphometric factors influencing the susceptibility to flooding (lowest and flattest areas) provide information of areas that might be affected by flooding due to their morphometric properties

at the Algerian coast where sea waves intruded several km landward (Fig. 10.14). In case of the Qued Lekbir traces of high energetic flood waves are clearly visible on satellite images with arrow-like shaped, parallel debris-walls, intersecting each other, directed towards SE. When merging the satellite images (Sentinel 2 and Landsat 8) with ASTER DEM data, the areas susceptible to flooding can be visualized. Areas with height levels below 10 m clearly show traces of previous flooding events like residual ponds. Further on, areas below 20 m are prone to flash floods in case of high precipitations as well.

The return flow (backwash) after tsunami or storm surge flooding has to be monitored. In general, the return current flows into the low-elevated areas or into river beds and channels, sometimes partly remaining there for days before discharging back into the sea, leading to the salinization of groundwater and of soils.

A systematic inventory of backwater areas, of coast-near lakes and ponds and their seasonal water level and volume changes as a prerequisite for flooding preparedness can be carried out as well with the support of remote sensing. With regard to climate change the monitoring of those seasonal changes (water volume, outline, etc.) gets an increasing importance. When high energetic flood waves intrude landwards during a humid season with high water levels in the lakes and ponds the extent
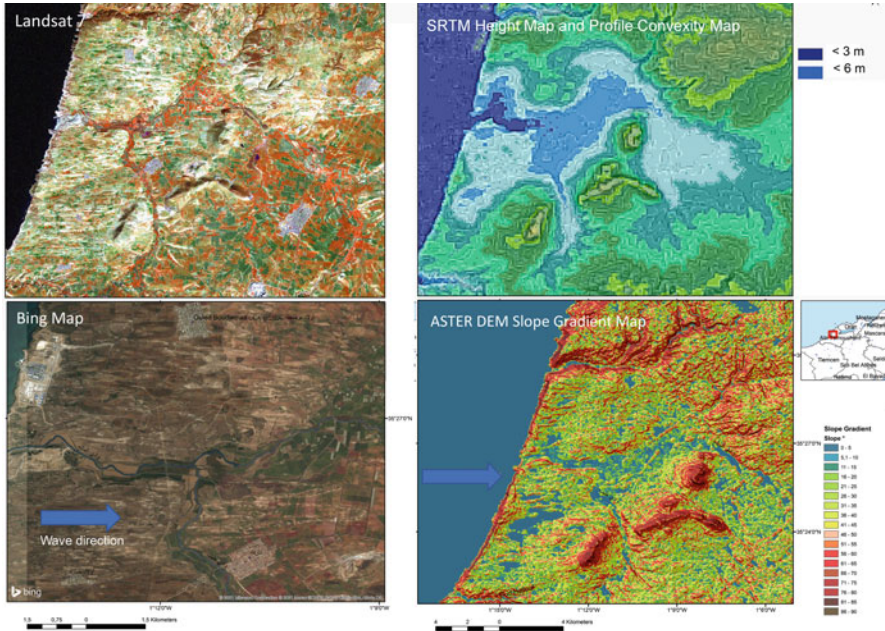
Fig. 10.16 Traces of flood waves more than 12 km landward visible on satellite data of the Algerian west coast, the sandy material later affected by eolian activity (erosion and sedimentation)

of flooded areas will be larger than during a dry season with low water levels or dried-up streams and lakes. This is demonstrated by the example from the coastal area in the east of the city Annaba in NE-Algeria (Fig. 10.17). Whereas the lowlands are nearly dried during the summer, they are partly flooded during the humid season in wintertime. The resulting map of the weighted overlay approach (merging and summarizing the morphometric factors influencing the disposition to flooding) shows in dark-blue colours those areas with the highest susceptibility to flooding in case of flash floods or tsunami flooding.

Height level maps indicating those areas below 10 m height level help to identify areas at risk such as in the next figures from Algiers. Merging height level data with actual satellite images show the infrastructure prone to potential flooding (Figs. 10.18a and 10.18b).

The weighted overlay approach in ArcGIS can contribute to the detection of those lowlands, that after the return-flow could remain longer time flooded than the environment. The result of a weighted overlay of morphometric factors in ArcGIS influencing the susceptibility to flooding is shown in the next figure of the Bay of Algiers (Fig. 10.19). Even in longer distances from the shoreline flooding might be possible affecting the southern city area of Algiers.

GEBCO bathymetric data were used to derive hillshade and flow accumulation maps (Fig. 10.20, image above) to localize canyons along the coast. The Algerian
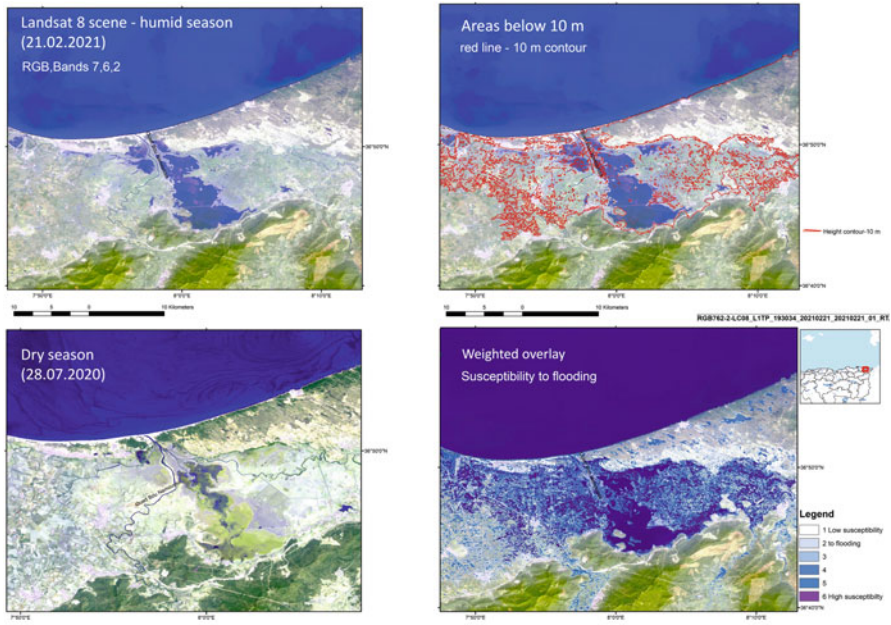
Fig. 10.17 Seasonal variability of the flooding extent influencing the additional flooding in case of tsunami events
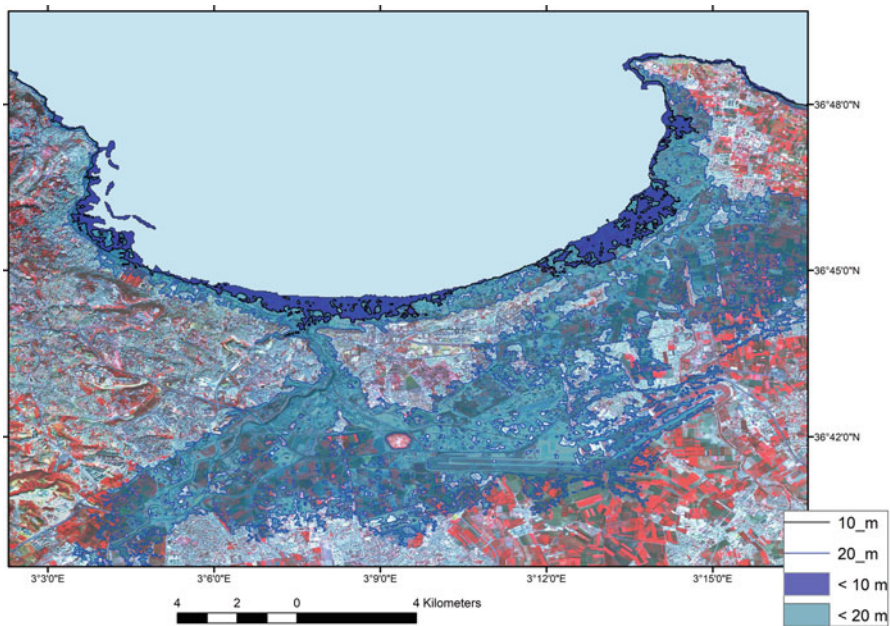

Fig. 10.18a Sentinel 2 scene (31.10.2020) merged with ASTER DEM data below 10 m and 20 m height level
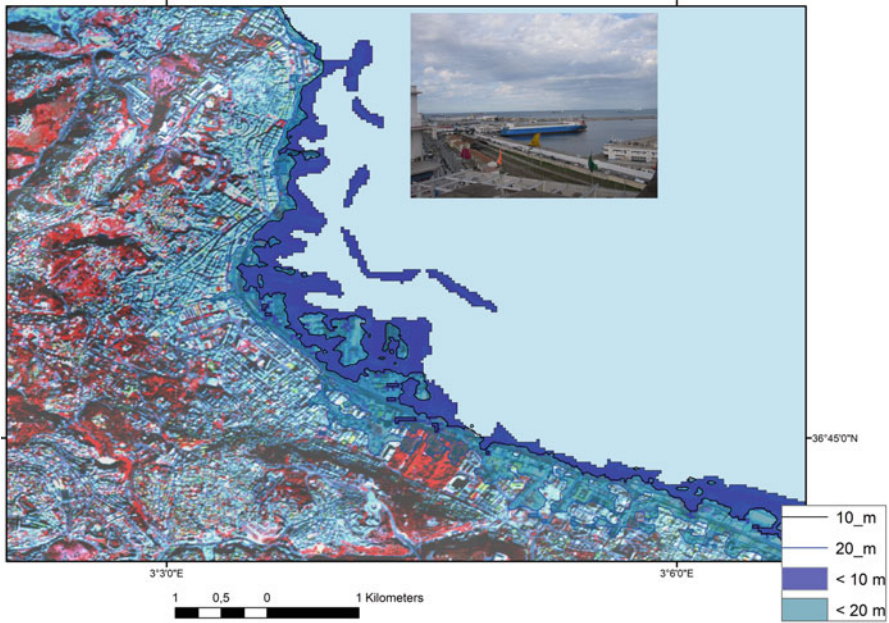
Fig. 10.18b Sentinel 2-scene merged with height level data below 10 m in the western Bay of Algiers (image of the harbour: Theilen-Willige, taken 2014)
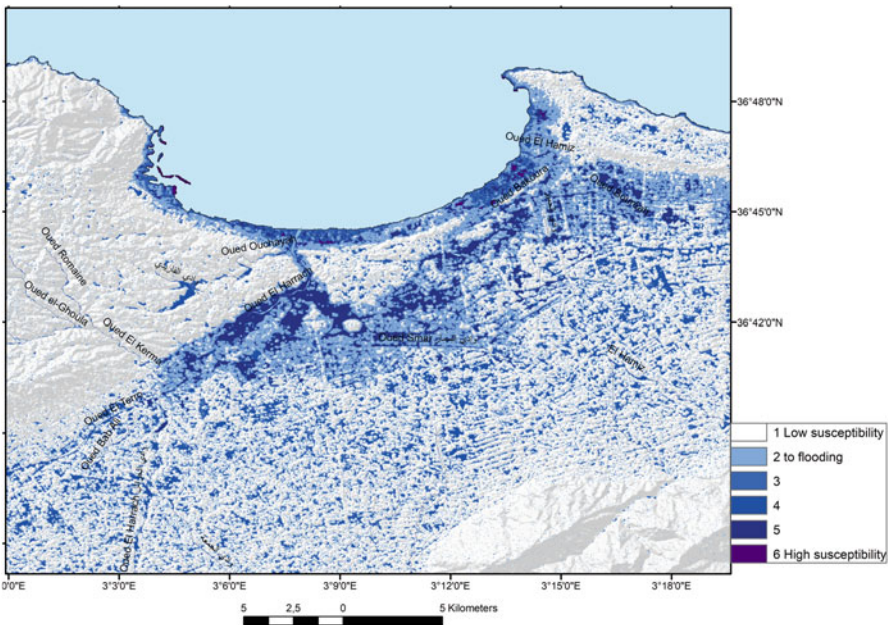

Fig. 10.19 Weighted overlay of morphometric factors to visualize areas susceptible to flooding in case of flash floods and tsunami waves in the coast-near part in the area of Algiers based on ASTER DEM data (30 spatial resolution)
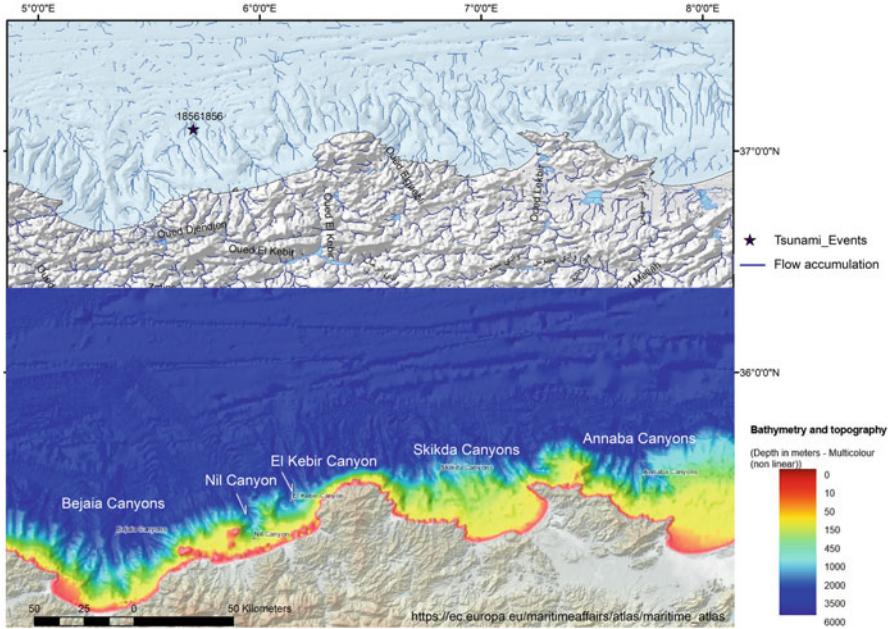
Fig. 10.20 The role of canyons along the Algerian coast in case of high energetic flood waves from northern direction by focusing wave energy
The blue lines in the map above are derived from the flow accumulation calculation in ArcGIS based on GEBCO bathymetric data. The lower map was provided by the European Atlas of the Seas/European Commission

continental shelf is relatively narrow, 5–10 km wide on average (Cattaneo et al., 2012). The continental slope along the Algerian coast is irregular, with intermediate flats of various width and a rather sinuous slope breaks (Domzig et al., 2006). The morphology of the continental slope of central Algeria presents abrupt scarps that at least partly correspond to active tectonic structures.

In case of significant tsunami occurrence from northern direction these canyons oriented perpendicular towards the coast could focus wave energy within these canyons which might lead in a worst case scenario to a higher flooding extent along the affected coast segments. Deep submarine canyons can lead to the amplification of waves on both sides of the canyons. The width length, and depth of the canyons play a role as well as the width of the shelf area. The effect of the parallel, NW-SE, to N-S-oriented arrangement of the canyons perpendicular to the coast has to be taken into account as well.

Tsunami wave propagating through submarine canyons has been studied by Jinadasa (2008) and Ioualalen et al. (2007), who analyzed the effect of 2004 Indian Ocean Tsunami in Sri Lanka and Bangladesh, respectively. The former found that the maximum inundation occurred just in front of the submarine canyons. In a similar manner, the latter found that the waves were amplified near the coast

(Aranguiz & Shibayama, 2013). In addition tsunami wave heights could be further enhanced due to overlapping of incoming waves with reflected waves from the coastal area. Tidal effects are a potential further source to increase tsunami heights up to a few centimeters (Jinadasa, 2008). Thus, the effect of the tide when investigating tsunami hazard, particularly, in coasts where tidal variations are significant has to be considered.

The next figures present examples of coast segments where submarine valleys are oriented in the same direction as the rivers along the coast (Figs. 10.21, 10.22 and 10.23). River mouths of rivers with the same orientation as the canyons along the coast might be exposed to focused wave energy due to funneling effects. In case of high energetic waves such as tsunami waves or landslide-tsunamis from northwestern and northern direction, the river mouths, especially those with the same orientation as of submarine valleys and canyons, could form an entrance for the flood waves and, thus to extended flooded areas.

The behavior of tsunami waves propagating over submarine canyons along the Algerian coast could also be influenced by abrupt changes in bathymetry, such as those caused by the steep continental slope with height differences of about 3000 m, see Fig. 10.21.
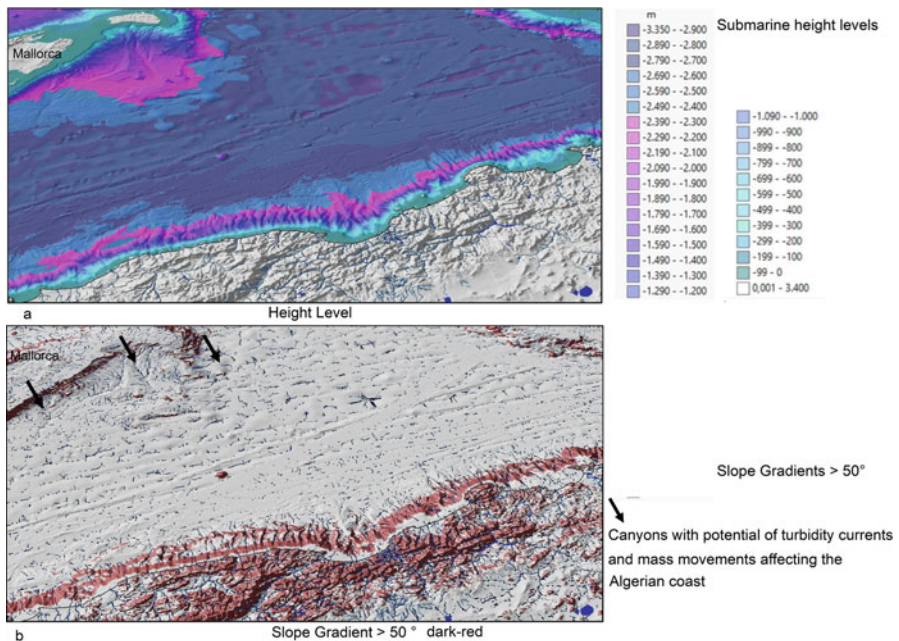

Fig. 10.21 3D perspective view of the Algerian coast based on GEBCO bathymetric data
(**a**) Height level
(**b**) Slope gradients > 50° combined with flow accumulation calculations to visualize potential valley and canyon sites prone to submarine turbidity currents
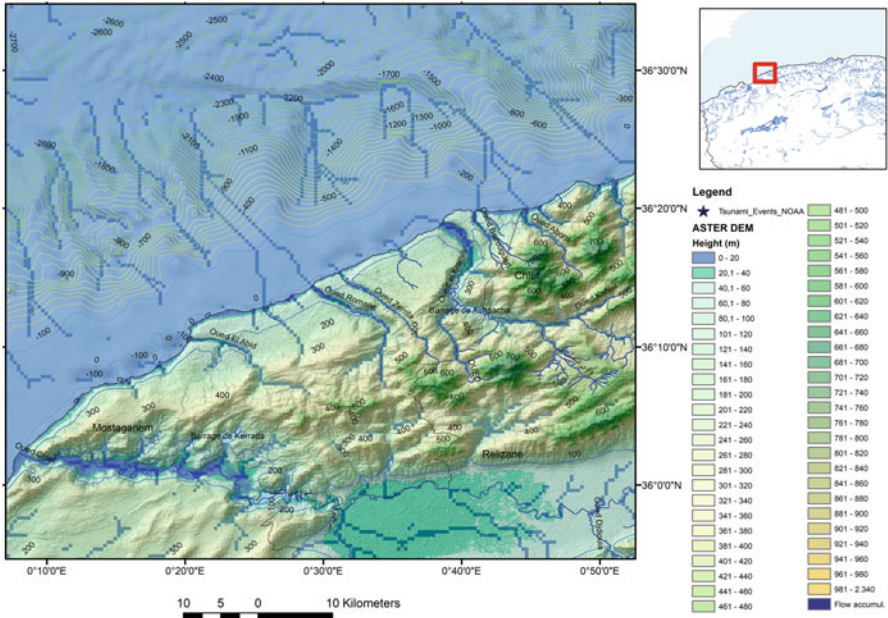
Fig. 10.22 River mouths and oriention of the rivers with the same NW-SE orientation of canyons along the coast
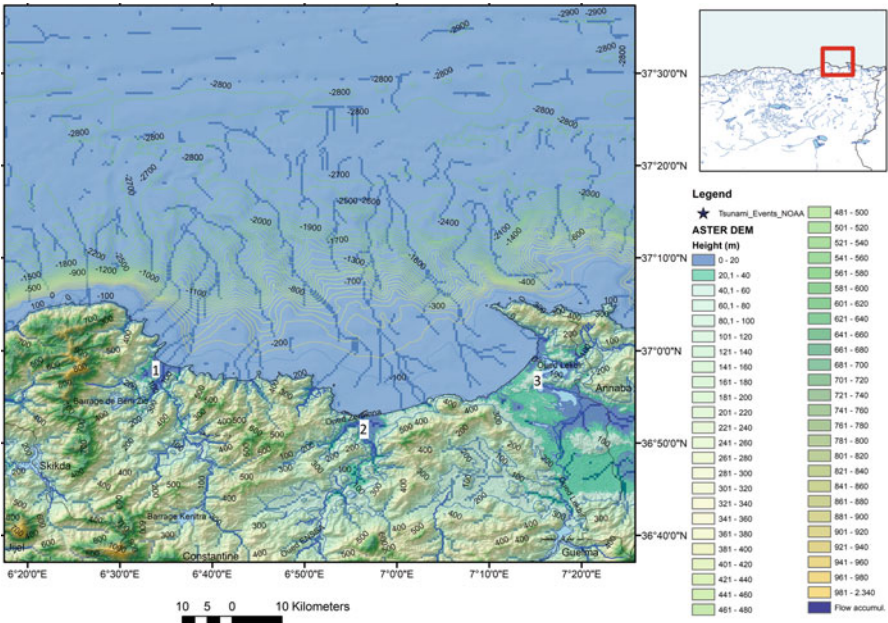

Fig. 10.23 River mouths and oriention of the rivers with the same NNW-SSE orientation of canyons along the coast of Collo and Skikda with exposure of Qued Elguebli (1) in the western part, Qued Zeramna (2) in the central part and Qued Lekbir (3) in the eastern part of the scene

Whenever the sources and main directions of tsunami waves or meteotsunamis are known, a warning should be given especially to those settlements within larger river mouth situated in areas below 10 m height levelt hat are exposed to the main wave fronts. The height levels have to be adapted and modified, however, in future according to sea level rise changes.

10.4 Conclusions

The input of remote sensing and GIS can be considered only as a small part of the whole "mosaic" of flooding susceptibility research approaches. Nevertheless, it offers a low-cost to no-cost approach (as the used DEM and satellite data are free), that can be used in any area, providing a first basic data stock for emergency preparedness by including susceptibility-to-flooding maps.

Summarizing factors influencing flooding susceptibility such as relatively low height levels (<10 m), terrain curvature (values calculated in ArcMap = 0, corresponding to flat terrain), slope gradients <10°, drop raster <50.000, and high flow accumulation values by using the weighted-overlay tools in ArcGIS, help to detect areas with higher flooding susceptibility due to their geomorphologic disposition. Due to the aggregation of causal, morphometric factors, those areas can be visualized. This approach is suited to obtain a first basic overview on susceptible areas according to a standardized approach. This might be of interest especially for countries with low financial resources wherein such maps are still unavailable.

The impact of storm surge or tsunami waves on the coast depends on geomorphological settings of the coast as well as the shelf (Abdul Rasheed et al., 2006). Variation in run-up along the coastline depends on the topography of the coastline, near-shore bathymetry, beach slope, coastal orientation, direction of the arriving wave etc. Variations in the near shore bathymetry and bottom topography were be studied to understand the relationship with the amplification of tsunami height development. The evaluations of bathymetric data reveal the steep submarine slopes in front of the Algerian coast and the submarine valleys and canyons perpendicular to the coast line. Depending on the source of high energetic waves and wave angle a focusing effect of the canyons on wave energy is possible.

Satellite images contribute to a better understanding of the interactions between the coastal morphology on the development of water currents, of course depending on meteorologic and tidal conditions at the acquisition time of the images.

Based on DEM and different satellite data, as well as infrastructural data those settlements and cities situated in lowlands and river mouth areas can be identified and integrated into a disaster management system (Fig. 10.24). When creating buffer zones with a 2 km-radius along the river mouth areas and intersecting these buffer zones with known settlements and cities within theses buffer zones the potentially affected settlements can be identified. In case of emergency help could be better focused, coordinated and organized according to the size of the population.
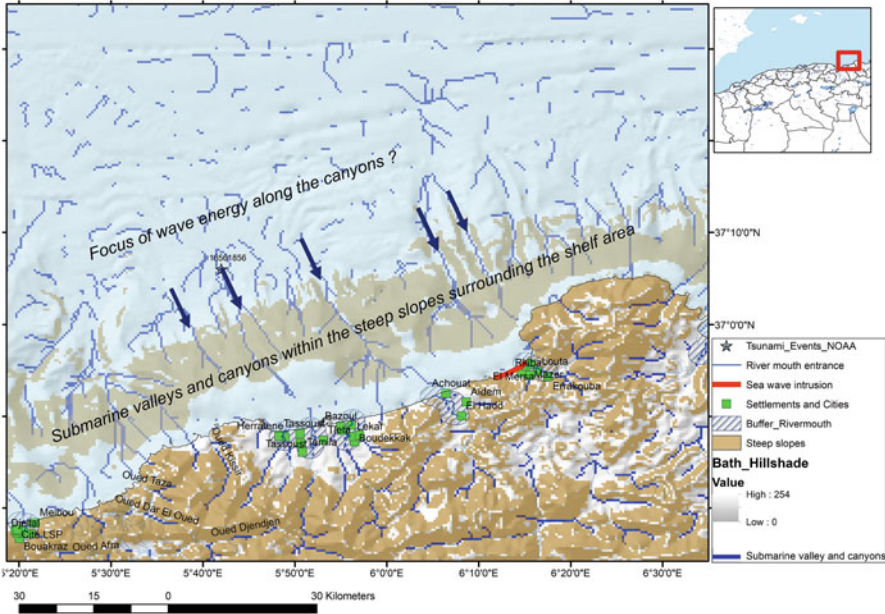
Fig. 10.24 Cities and settlements situated within a 2 km-radius-buffer zone along river mouth areas of rivers oriented in the same direction as the submarine canyons and valleys (see arrows)

It must be added that storm surges or meteo-waves, although generally not as destructive as a major tsunami-waves, can be comparatively more frequent. Therefore, inundation maps indicating the extent of the coastal area that could be affected by potential events of both tsunami waves, storm surges and flash floods should an input in any data base dealing with flooding hazards. The influence of sea-level rise due to climatic change has to be considered as well.

References

Abdul Rasheed, K. A., Kesava Das, V., Revichandran, C., Vijayan, P. R., & Thottam, T. J. (2006). Tsunami impacts on morphology of beaches along South Kerala coast, west coast of India. *Science of Tsunami Hazards, 24*(1), 24–34.

Alaska Satellite Facility (ASF). https://search.asf.alaska.edu/#/. Accessed 20 Nov 2020.

Alasset, P.-J., Hebert, H., Maouche, S., Calbini, V., & Meghraoui, M. (2006). The Tsunami induced by the 2003 Zemmouri earthquake (Mw=6.9): Modelling and results. *Geophysical Journal International, 166*, 213–226.

Ambraseys, N. N., & Vogt, J. (1988). Material for the investigation of the seismicity of the region of Algiers. *European Earthquake Engineering, 3*, 16–29.

Amir, L. (2014). Tsunami Hazard assessment in the Alboran Sea for the Western coast of Algeria. *Journal of Shipping and Ocean Engineering, 4*, 43–51.

Amir, L. A., & Theilen-Willige, B. (2017). Coastal risk and water flow analysis in Eastern Algeria (Western Mediterranean). *Universal Journal of Geoscience, 5*(4), 99–111. https://doi.org/10.13189/ujg.2017.050403

Amir, L., Cisternas, A., Vigneresse, J.-L., Dudley, W., & Mc Adoo, B. (2012). Algeria's vulnerability to tsunamis from near-field seismic sources. *Science of Tsunami Hazards, Journal of Tsunami Society International, 31*(1), 82–98.

Aranguiz, R., & Shibayama, T. (2013). Effect of submarine Canyons on Tsunami wave propagation: A case study oft he Biobio Canyon, Chile. *Coastal Engineering Journal, 55*(4), 1350016. https://doi.org/10.1142/S0578563413500162. (23 pages).

Beccario, C. (2020). *Earth – A visualization of global weather conditions forecast by supercomputers updated every three hours*. https://earth.nullschool.net/

Cattaneo, A., Babonneau, N., Ratzov, G., Dan-Unterseh, G., Yelles, K., Bracène, R., Mercier de Lépinay, B., Boudiaf, A., & Déverchère., J. (2012). Searching for the seafloor signature of the 21 May 2003 Boumerdes earthquake offshore central Algeria. *Natural Hazards and Earth System Sciences, 12*, 2159–2172. www.nat-hazards-earth-syst-sci.net/12/2159/2012/. https://doi.org/10.5194/nhess-12-2159-2012

Deverchere, J., Yelles, K., Domzig, A., Mercier de Lepinay, B., Bouillin, J.P., Gaulier, V., Bracene, R., Calais, E., Savoye, B., Kherroubi, A., Le Roy, P., Pauc, H., & Dan, G. (2005). Active thrust faulting offshore Boumerdes, Algeria, and its relation to the 2003 Mw 6.9 earthquake. *Geophysical Research Letters, 32*. https://doi.org/10.1029/2004GL021646

Domzig, A., Yelles, K., Le Roy, C., Déverchère, J., Bouillin, J.-P., Bracène, R., Mercier de Lépinay, B., Le Roy, P., Calais, E., Kherroubi, A., Gaullier, V., Savoye, B., & Pauc, H. (2006). Searching for the Africa–Eurasia Miocene boundary offshore western Algeria (MARADJA'03 cruise). *Comptes rendus geoscience, 338*, 80–91. https://doi.org/10.1016/j.crte.2005.11.009

EMODnet Bathymetry Consortium. (2020). EMODnet Digital Bathymetry (DTM). https://doi.org/10.12770/bb6a87dd-e579-4036-abe1-e649cea9881a

European Environment Agency. https://www.eea.europa.eu/data-and-maps/indicators/sea-level-rise-7/assessment. Accessed 05 Jan 2021.

European Space Agency (ESA). https://scihub.copernicus.eu. Accessed 15 Feb 2021.

Gelfenbaum, G. (2005). Coastal currents. In M. L. Schwartz (Ed.), *Encyclopedia of coastal science* (Encyclopedia of Earth Science Series). Springer. https://doi.org/10.1007/1-4020-3880-1_78

General Bathymetric Chart of the Oceans (GEBCO). https://www.gebco.net/https://www.gebco.net/data_and_products/gebco_web_services/web_map_service/mapserv? Accessed 17 Nov 2020.

Gusiakov, V. K. (2020). Global occurrence of large tsunamis and tsunami-like waves within the last 120 years (1900–2019). *Pure and Applied Geophysics, 177*, 1261–1266. https://doi.org/10.1007/s00024-020-02437-9

Ioualalen, M., Pelynovsky, E., Asavanant, J., Lipikorn, R., & Deschamps, A. (2007). On the weak impact of the 26 Indian Ocean tsunami on the Bangladesh coast. *Natural Hazards and Earth System Sciences, 7*, 141–147.

Jinadasa, S. U. P. (2008). *Interaction of tsunami wave propagation with coastal bathymetry and geomorphology: A case study in Sri Lanka*. General Bathymetric Chart of the Oceans (GEBCO) Science Day 2008, Japan Coast Guard, Tokyo, Japan.

Lopez Marinas, J. M., & Salord, R. (1990). *El periodo sismico oranes de 1790 a la luz de la documentación de los archivos espanoles*. I.G.N. Publication, 6, 64 pages. Madrid.

Monserrat, S., Vilibic, I., & Rabinovich, A. B. (2006). Meteotsunamis: Atmospherically induced destructive ocean waves in the tsunami frequency band. *Natural Hazards and Earth System Sciences, 6*, 1035–1051. www.nat-hazards-earth-syst-sci.net/6/1035/2006/.

Papadopoulos, G. A., & Fokaefs, A. (2005). Strong tsunamis in the Mediterranean Sea: A re-evaluation. *ISET Journal of Earthquake Technology, 463*(42, 4), 159–170.

Papadopoulos, G. A., Daskalaki, E., & Fokaefs, A. (2007). Tsunamis generated by coastal and submarine landslides in the Mediterranean Sea. In V. Lykousis, D. Sakellariou, & J. Locat (Eds.), *Submarine mass movements and their consequences* (pp. 415–422). Springer. https://doi.org/10.1007/978-1-4020-6512-5_43

Pleskachevsky, A., Jacobsen, S., Tings, B., & Schwarz, E. (2019). Estimation of sea state from Sentinel-1 synthetic aperture radar imagery for maritime situation awareness. *International Journal of Remote Sensing, 40*(11), 4104–4142. https://doi.org/10.1080/01431161.2018.1558377

Shao, W., Zhang, Z., Li, X., & Li, H. (2016). Ocean wave parameters retrieval from Sentinel-1 SAR imagery. *Remote Sensing, 8*, 707. https://doi.org/10.3390/rs8090707

Soloviev, S. L., Solovieva, O. N., Go, C. N., Kim, K. S., & Shchetnikov, N. A. (2000). *Tsunamis in the Mediterranean Sea, 2000 B.C.–2000 A.D. Advances in natural and technological hazards research* (p. 260). Kluwer Academic Publishers.

Theilen-Willige, B. (2006). Emergency planning in northern Algeria based on remote sensing data in respect of Tsunami Hazard preparedness. *Science of Tsunami Hazards, 25*(1), 3–18.

US Geological Survey (USGS)/Earth Explorer. https://earthexplorer.usgs.gov/. Accessed 12 Dec 2020.

Yelles-Chaouche, A., Roger, J., Déverchère, J., Bracène, R., Domzig, A., Herbert, H., & Kherroubi, A. (2009). The 1856 Tsunami of Djidjelli (Eastern Algeria): Seismotectonics, modelling and hazard implications for the Algerian Coast. *Pure and Applied Geophysics, 166*, 283–300. Basel: Birkhäuser Verlag, 0033–4553/09/010283–18, https://doi.org/10.1007/s00024-008-0433-6

Yelles, A. K., Lammali, K., Mahsas, A., Calais, E., & Briole, P. (2004). Coseismic deformation of the 21st May 2003, Mw = 6.8 Boumerdes earthquake, Algeria, from GPS measurements. *Geophysical Research Letters, 31*. L13610, https://doi.org/10.1029/2004GL019884